Acupuncture and Herbal Medicine

Effect of moxibustion on P2X7R/NF-κB pathway in ulcerative colitis rats with repeated induction of DSS

Zhe Ma[1,2], Lingjie Li[1,3], Huangan Wu[1,2,*], Jianhua Zhou[4], Yaying Lin[1,2], Yu Qiao[1,2], Shiyu Zheng[1,2], Ling Yang[1,2], Yan Huang[1,2], Yanan Liu[1,2], Fang Zhang[1,2], Lu Zhu[1,2], Qin Qi[1,2], Luyi Wu[1,5,*]

[1]Yueyang Hospital of Integrated Traditional Chinese and Western Medicine, Shanghai University of Traditional Chinese Medicine, Shanghai, China; [2]Shanghai Research Institute of Acupuncture and Meridian, Shanghai, China; [3]Shanghai Municipal Hospital of Traditional Chinese Medicine, Shanghai University of Traditional Chinese Medicine, Shanghai, China; [4]Shanghai Eighth People's Hospital, Shanghai, China; [5]Shanghai University of Traditional Chinese Medicine, Shanghai, China

Abstract

Objective: To investigate the mechanism by which moxibustion regulates the expression of inflammatory cytokines in ulcerative colitis (UC) rats through the P2X7 receptor (P2X7R)/nuclear factor-kappa B (NF-κB) pathway.

Methods: UC was induced using dextran sulfate sodium (DSS) in both wild-type (WT) and P2X7R knockout (KO) mice. General health conditions, pathological changes, and periodic acid-Schiff (PAS) staining of the colonic tissues were analyzed. Immunohistochemistry was used to detect NF-κB p65 protein expression in colonic tissues. Male Sprague-Dawley (SD) rats were randomly assigned to four groups: normal, model, normal + herb-partitioned moxibustion, and model + herb-partitioned moxibustion. UC was induced in rats by cyclic DSS administration. Rats in the herb-partitioned moxibustion group received moxibustion at the bilateral Tianshu (ST25) and Qihai (RN6) acupoints. The effects of herb-partitioned moxibustion were evaluated regarding general health conditions and histopathological alterations in colon tissue. The protein expression of P2X7R and NF-κB p65 in colonic tissues was determined by immunohistochemistry, whereas interleukin (IL)-10 mRNA levels were quantified using real-time quantitative polymerase chain reaction (RT-qPCR). Furthermore, enzyme-linked immunosorbent assay (ELISA) was used to measure serum concentrations of tumor necrosis factor-alpha (TNF-α) and IL-6.

Results: Colonic epithelial damage and inflammatory cell infiltration were significantly reduced in P2X7R KO mice compared to WT mice, along with reduced expression of NF-κB p65 protein in colonic tissues ($P < 0.05$). Moxibustion improves histopathological damage, goblet cell number, and intestinal mucus secretion in rats with UC. Compared to the normal group, the model group exhibited increased histopathological scores, serum TNF-α, and IL-6 levels, as well as elevated P2X7R and NF-κB p65 protein expression in colonic tissues ($P < 0.05$). In comparison to the model group, the model + herb-partitioned moxibustion group demonstrated significantly lower histopathological scores, reduced serum TNF-α and IL-6 levels, and decreased P2X7R and NF-κB p65 protein expression ($P < 0.05$).

Conclusions: Moxibustion at "Tianshu" and "Qihai" acupoints may inhibit the levels of IL-6 and TNF-α inflammatory factors and reduce inflammation in the UC colonic mucosa by regulating the P2X7R/NF-κB p65 pathway in UC colonic tissues.

Keywords: Immunomodulation, Moxibustion, NF-κB p65, P2X7R, Ulcerative colitis

Graphical abstract: https://links.lww.com/AHM/A177

Introduction

Ulcerative colitis (UC) is a chronic inflammatory condition classified under inflammatory bowel disease (IBD), primarily affecting the mucosal lining of the colon and rectum, the hallmark of UC is the presence of continuous and diffuse inflammation[1]. UC clinically manifests as intestinal symptoms, including abdominal pain, diarrhea, and the passage of mucus and blood, all of which reflect underlying mucosal inflammation and injury. In some cases, patients also experience extraintestinal complications affecting the skin, eyes, joints, or hepatobiliary system[2]. Global epidemiological surveys estimate that the prevalence of UC will reach approximately 5 million cases worldwide by 2023. It continues

Zhe Ma and Lingjie Li contributed equally to this work.

**Corresponding author. Luyi Wu, E-mail: luyitcm@163.com; Huangan Wu, E-mail: wuhuangan@126.com.*

Received 12 November 2024 / Accepted 8 May 2025

How to cite this article: Ma Z, Li LJ, Wu HG, Zhou JH, Lin YY, Qiao Y, Zheng SY, Yang L, Huang Y, Liu YN, Zhang F, Zhu L, Qi Q, Wu LY. Effect of moxibustion on P2X7R/NF-κB pathway in ulcerative colitis rats with repeated induction of DSS. Acupunct Herb Med 2025;5(2):205–216. doi: 10.1097/HM9.0000000000000159

Copyright © 2025 Tianjin University of Traditional Chinese Medicine. This is an open-access article distributed under the terms of the Creative Commons Attribution-Non Commercial-No Derivatives License 4.0 (CCBY-NC-ND), where it is permissible to download and share the work provided it is properly cited. The work cannot be changed in any way or used commercially without permission from the journal.

to rise in developing regions, posing an increasing burden on healthcare resources[3–5]. The etiology of UC remains elusive and may involve complex interactions between genetic susceptibility, compromised intestinal epithelial barrier integrity, dysregulated immune responses, and imbalanced microbiota[4]. UC is associated with a high recurrence rate, chronic disease progression, and an elevated risk of malignant transformation[6], underscoring the importance of deeper exploration into its pathogenesis and the discovery of more effective therapeutic targets.

Currently, pharmacological management, including using 5-aminosalicylic acid drugs, corticosteroids, and thiopurines, remains the cornerstone of UC treatment. The emergence of biologics and small-molecule drugs has shifted the treatment goals from symptomatic control to achieving complete clinical and endoscopic remission. Histological healing has emerged as a novel therapeutic benchmark[7]. However, despite these advancements, no existing treatment has completely cured UC. In recent years, acupuncture and moxibustion have demonstrated significant safety and efficacy in treating UC, with advantages such as reduced recurrence rates and sustained long-term benefits. Our research group has actively explored moxibustion's potential mechanisms and clinical applications for UC, confirming its regulatory effects on immune balance, improvement of mucosal lesions in the intestine, and suppression of intestinal inflammation[8–12]. However, the precise mechanisms underlying the therapeutic effects of moxibustion in UC remain unclear.

The P2X7 receptor (P2X7R), a subtype of purinergic receptor predominantly expressed on epithelial cells and various immune cells, is critically implicated in inflammatory processes[13–15]. Animal models have demonstrated that the activation of P2X7R with agonists in a TNBS-induced colitis model significantly exacerbates inflammation, whereas antagonizing P2X7R markedly attenuates inflammation[16]. Nuclear factor-kappa B (NF-κB) is a pivotal regulator in the transcriptional control of genes related to immunity, inflammation, and cell death[17]. As a downstream target of P2X7R, NF-κB functions as a critical regulator of inflammation, driving the transcription of cytokines and other inflammatory mediators; P2X7R activation triggers NF-κB signaling, thereby amplifying inflammatory cascades[18]. The P2X7R/NF-κB pathway has gained recognition for its potential involvement in the pathogenesis of UC, however, further research is essential to fully delineate its precise mechanisms and therapeutic implications. Our earlier investigations have indicated that acupuncture and moxibustion could alleviate dextran sulfate sodium (DSS)-induced acute colonic inflammation *via* the P2X7R-NLRP3 inflammasome signaling pathway[19]. This study used P2X7R knockout (KO) mice to investigate their role in UC pathogenesis. Furthermore, using a DSS-induced UC rat model to simulate recurrent colitis episodes, we aimed to clarify whether moxibustion exerts anti-inflammatory effects by modulating the P2X7R/NF-κB axis and regulating inflammatory factors in colonic tissue. This approach provides insights into the therapeutic mechanisms of moxibustion in UC.

Materials and methods

Experimental drugs and reagents

Pentobarbital sodium: Sigma-Aldrich (P3761, St. Louis, MO, USA); Hematoxylin-Eosin Stain kit: Nanjing Jiancheng Technology Co., Ltd (D006-1-1); Periodic Acid-Schiff (PAS) dye kit: Servicebio (G1008-20ML); Anti-P2RX7 antibody: Abcam (ab109054); Anti-NF-κB p65 antibody: CST (8242s); dextran sodium sulfate (DSS): MP Biomedicals 36000-50000 (0216011090); tumor necrosis factor-alpha (TNF-α) and interleukin (IL)-6 rat enzyme-linked immunosorbent assay (ELISA) Kits: Shanghai Wei Ao Biotechnology Co., Ltd (ER20497M; ER20298M).

Experimental animals

Twenty-eight male Sprague-Dawley (SD) rats and 24 male mice—comprising 12 C57BL/6J wild-type (WT) mice obtained from Shanghai Slack Laboratory Animal Co., Ltd., and 12 P2X7R KO mice procured from The Jackson Laboratory (USA)—were utilized. All experimental animals were maintained at Shanghai University of Traditional Chinese Medicine's Laboratory Animal Facility under a regulated 12-hour light/dark cycle, consistent temperature of (20 ± 2) °C, and humidity levels ranging from 50% to 70%, ensuring minimal environmental variability and optimal experimental conditions. Experimental animals underwent a 1-week acclimation period to standardize physiological and behavioral parameters before the initiation of experimental procedures, thereby ensuring consistent and reliable baseline conditions. All animal procedures performed in this study were reviewed, approved, and supervised by the Animal Ethics Committee of Shanghai University of Traditional Chinese Medicine, ensuring strict adherence to ethical standards and animal welfare guidelines (Approval number: PZSHUTCM211227012).

Grouping and model preparation

In this experiment, WT and P2X7R gene KO mice were employed initially to determine the contribution of P2X7R signaling to inflammation modulation in an experimental UC model. Mice were randomly assigned to four experimental groups (n = 6 each): wild-type normal control (WT-NC), wild-type UC model (WT-UC), P2X7 receptor knockout normal control (P2X7R KO-NC), and P2X7 receptor knockout UC model (P2X7R KO-UC). The UC model was established through continuous oral administration of a 3% DSS aqueous solution for 7 days in WT-UC and P2X7R KO-UC groups[20].

Subsequently, observe the mechanism of action of moxibustion intervention on the P2X7R/NF-κB pathway in UC rats. Using a completely randomized design, SD rats were allocated into two equal groups: the NC group (n = 14) and the colitis model group (n = 14). The UC rat model was established using a cyclic drug administration following the protocol described by Greten et al.[21], with slight modifications consisting of the following steps: rats in the modeling group underwent three cycles of inflammatory stimulation. During cycle 1, the rats received 3% DSS solution for 4 days, followed by normal drinking water for 17 days. In cycle 2, a 2% DSS solution was administered for 4 days, followed by normal drinking water for 17 days. Finally, in

cycle 3, the rats were treated with 2% DSS solution for 4 days, followed by normal drinking water for 10 days until the end of the modeling period (Figure 1A). At the end of the modeling phase, two rats from each of the normal and modeling groups were randomly selected for model evaluation. The histopathological observation of the ulcerated surfaces confirmed the model's success using hematoxylin and eosin (HE) staining. After confirming successful modeling, rats from the modeling group were randomly assigned to one of two subgroups: a model group and a model + herb-partitioned moxibustion group, with six rats in each (n = 6). Similarly, rats from the normal group were separated into two subgroups: a normal group and a normal + herb-partitioned moxibustion group, also consisting of six rats per group (n = 6). The intervention phase began immediately after the establishment of the UC model. Rats belonging to the normal + herb-partitioned moxibustion group and those in the model + herb-partitioned moxibustion group subjected to the same treatment received moxibustion therapy.

Methods of moxibustion intervention

On the day following model establishment, the abdominal hair around the Tianshu (ST25) and Qihai (RN6) acupoints was shaved using specialized depilatory cream for experimental animals. Herb-partitioned moxibustion was commenced on the second day post-modeling. The medicinal cake is composed of Fuzi (*Radix Aconiti Lateralis Preparata*), Rougui (*Cortex Cinnamomi Cassiae*), Muxiang (*Radix Aucklandiae*), Huanglian (*Rhizoma Coptidis*), Honghua (*Flos Carthami*), Danshen (*Radix Salviae Miltiorrbizae*), and Danggui (*Radix Angelicae Sinensis*)[10]. The ingredients were prepared by mixing powdered herbs with yellow wine to create a disc-shaped mixture, measuring around 0.4 cm in thickness and approximately 0.8 cm across in diameter. To administer the moxibustion intervention, medicinal cakes were placed at the bilateral ST25 and RN6 acupoints. Afterward, a 90 mg moxa cone, sourced from Nanyang Hanyi Moxa Co., Ltd. (Nanyang, China), was carefully placed atop each medicinal cake and ignited. Each moxa cone maintained combustion for approximately 5 minutes, with two moxa cones applied to each acupoint per day for a continuous period of 10 days. The control groups (normal and model groups) did not receive herb-partitioned moxibustion but underwent similar handling and fixation to mimic the procedural conditions the treated groups experienced.

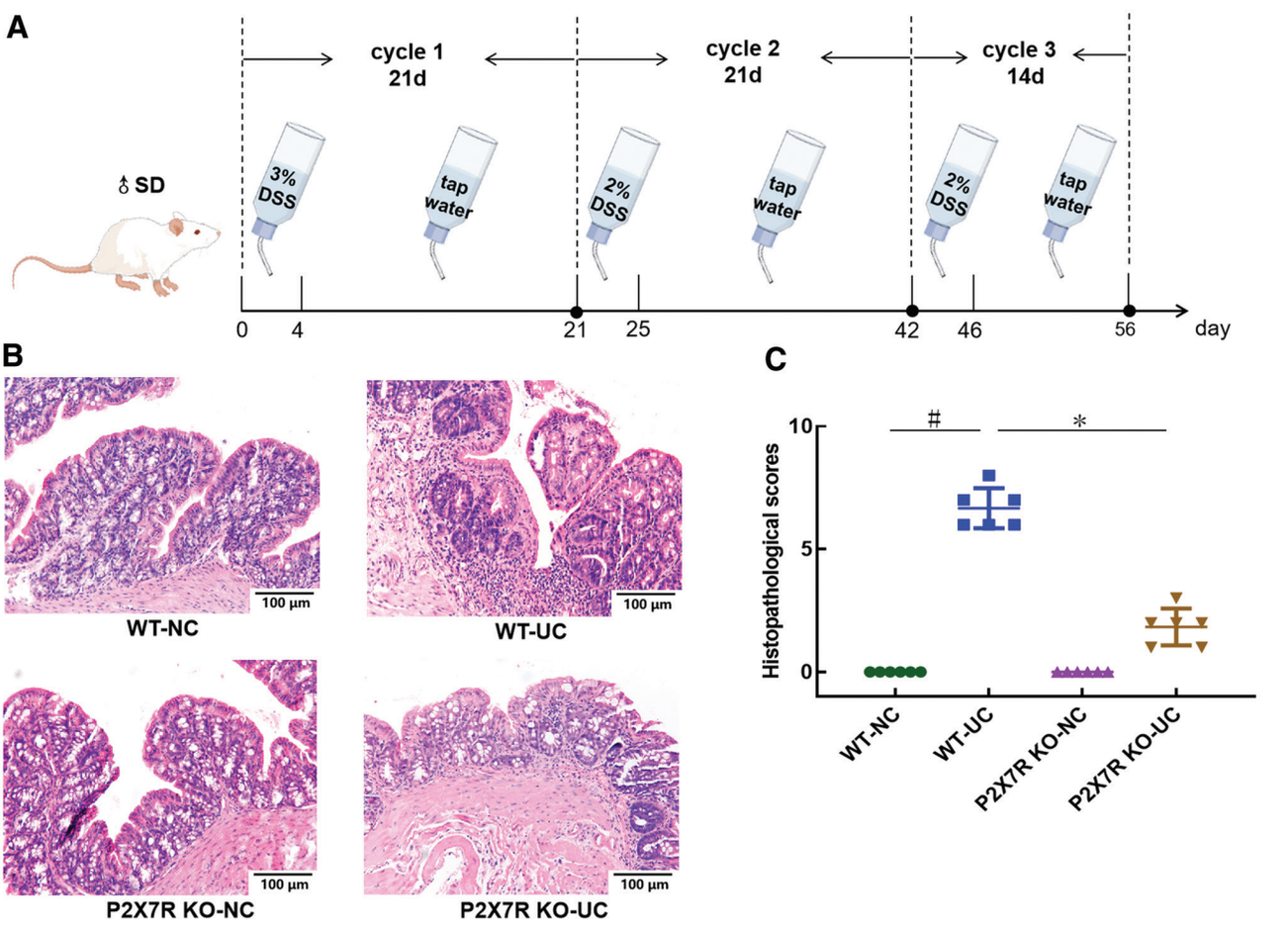


Figure 1. Schematic diagram of UC rat model preparation and effects of moxibustion on the histopathology of the colon in UC mice. (A) Schematic diagram of UC rat model preparation; (B) HE staining of mice colon tissue in each group. (C) Each group's histopathologic scores of mice colon tissue (median [P_{25}, P_{75}], n = 6). Compared with the WT-NC group, $^{\#}P < 0.05$; with the WT-UC group, $^{*}P < 0.05$. DSS: Dextran sulfate sodium; HE: Hematoxylin and eosin; P2X7R: P2X7 receptor; P2X7R KO-NC: P2X7R gene knockout normal group; P2X7R KO-UC: P2X7R gene knockout model group; SD: Sprague-Dawley; UC: Ulcerative colitis; WT-NC: Wild-type normal group; WT-UC: Wild-type model group.

Specimen collection and processing

Upon completing the intervention, anesthesia was induced in all rats through an intraperitoneal injection of 2% sodium pentobarbital (30–40 mg/kg). Carefully open the abdominal cavity, collect blood from the abdominal aorta, let it stand at room temperature for 2 hours, and then extract the serum by centrifugation (3,000 g, 15 minutes, 4°C). The colon was carefully cut open along the mesentery in a longitudinal direction and subsequently washed with saline solution. Two segments of colon tissue were taken from each animal: one segment was fixed in 4% paraformaldehyde fixative, the remaining portion was rapidly frozen using liquid nitrogen and preserved at –80°C for subsequent analysis.

Anesthesia was induced in the mice through an intraperitoneal injection of 1% pentobarbital sodium at a dosage of 40 to 50 mg/kg after drinking an aqueous DSS solution for 7 days. All procedures mirrored those used in rats; each segment was divided into two portions: one portion was preserved in paraformaldehyde for fixation, while the other portion was preserved at –80°C for subsequent analysis.

General condition observation

Monitor the general condition of the animals in each experimental group, including factors such as food consumption, water intake, mental state, fur luster, and stool characteristics.

Observation of colon histopathology

The tissue sections were subjected to a standard deparaffinization and rehydration protocol, beginning with immersion in xylene I and II for 20 minutes each to dissolve the paraffin. This was followed by sequential rehydration through a graded ethanol series with decreasing concentrations (100%, 95%, 90%, 80%, and 70%), with each step lasted 5 minutes to ensure thorough hydration and preparation for subsequent staining procedures. The sections were then immersed twice in double-distilled water for 5 minutes each. Hematoxylin staining was performed for 2 to 3 minutes, followed by thorough rinsing with running water for 10 minutes. The sections were briefly differentiated by immersion in 1% hydrochloric acid alcohol for 1 to 2 seconds, followed by another rinse under running water for an additional 5 minutes. Eosin staining was performed for 2 to 3 minutes before sequential dehydration using an ascending ethanol gradient (70%, 80%, 90%, and 100%) for 1 to 2 seconds per step. Transparency was achieved by immersing the sections in xylene I and II for 15 minutes, after which they were sealed. Colonic tissue morphology was observed under a light microscope, and histopathological damage was scored as previously described[22].

PAS staining of colon tissue

For PAS staining, the tissue sections underwent initial dewaxing using environmentally friendly reagents I and II, each applied for a duration of 20 minutes. Subsequently, dehydration was carried out with two successive treatments of absolute ethanol, each lasting 5 minutes, followed by a 5-minute immersion in 75% ethanol. After washing thoroughly with tap water, the tissue sections were incubated in PAS staining solution B for a period ranging between 10 and 15 minutes. After this staining phase, sections were gently washed first with tap water and then rinsed twice using distilled water. Subsequently, the samples were transferred into PAS solution A, where they remained for 25 to 30 minutes under light-protected conditions. This was followed by an additional 5-minute rinse under continuous flow of tap water. Following light hematoxylin counterstaining and differentiation with aqueous hydrochloric acid solution, the sections were subjected to ammonia-induced bluing, followed by sequential dehydration in anhydrous ethanol I, II, and III (5 minutes each). Sections were cleared twice with xylene (5 minutes each) before sealing. Goblet cell counts and mucosal mucus distribution within colonic tissues were examined using light microscopy.

Enzyme-linked immunosorbent assay

The concentrations of TNF-α and IL-6 in rat serum samples from each experimental group were quantitatively assessed using an ELISA. All reagents, calibration standards, and biological samples were prepared in accordance with the protocols specified by the reagent manufacturer. The steps of the assay were executed as follows:

1. Sample addition: A volume of 100 μL of standard solutions or experimental samples was dispensed into the designated wells of the microplate. The plate was then incubated at room temperature for 2.5 hours, after which it underwent thorough washing to remove unbound components.
2. Biotin-labeled antibody: One hundred microliters of biotin-labeled antibody was added to each well, incubated for 1 hour at room temperature with gentle shaking, and washed.
3. Primary antibody solution: Add 50 μL of distilled water and 50 μL of primary antibody working solution to each well (excluding the blank control). Mix thoroughly and incubate at 37°C for 20 minutes, followed by a plate wash.
4. Enzyme-labeled antibody: Add 100 μL of the prepared enzyme-labeled antibody solution to each well of the microplate. Incubate the plate at 37°C for a duration of 10 minutes to facilitate binding, followed by washing steps performed in accordance with the previously outlined protocol.
5. Substrate addition: Add 100 μL of the substrate solution to each designated well, and incubate the microplate at 37°C for 15 minutes under light-protected conditions.
6. Reaction termination: Add 100 μL of stop solution to each well, ensuring complete mixing to uniformly halt the enzymatic reaction.
7. Absorbance measurement: Within 30 minutes following termination of the reaction, the absorbance at 450 nm was determined using a calibrated microplate reader.

This step-by-step approach ensures precision and consistency in measuring TNF-α and IL-6 concentrations.

Immunohistochemical (IHC) method

IHC analysis was employed to evaluate the expression levels of P2X7 receptor and NF-κB p65 proteins in colonic tissues, following the protocol: deparaffinization and hydration of sections; antigen retrieval; blocking endogenous enzyme activity; incubation with primary

antibodies at 37°C followed by overnight refrigeration at 4°C; addition of secondary antibodies on a subsequent day; rinsing with phosphate-buffered saline (PBS); diaminobenzidine (DAB)-based chromogenic development; hematoxylin counterstaining; dehydration; clearing with xylene; and section sealing. Three to five random microscopic fields per section were photographed for quantitative analysis at consistent luminosity settings. The analysis of positive staining was conducted using Image-Pro Plus software (version 6.0), which was utilized to determine key parameters: the positive area (area), the integrated optical density (IOD), and the average optical density (AOD = IOD/area). These metrics were subjected to statistical analyses for inter-group comparisons.

Real-time quantitative polymerase chain reaction technology

Real-time quantitative polymerase chain reaction (RT-qPCR) was performed to detect IL-10 mRNA expression in rat colon tissues using the following steps: 1) total RNA extraction, 2) reverse transcription, and 3) fluorescence quantitative PCR amplification. The rat gene sequences were aligned based on the corresponding target gene entries available in the GenBank database. IL-10-F: CTGTCATCGATTTCTCCCCT; IL-10-R:CAAACTCATTCATGGCCTTG; GAPDH-F: GGCAAGTTCAACGGCACAGT;GAPDH-R:ATGACATACTCAGCACCGGC; reaction conditions: 95°C, 2 minutes; (94°C for 10 seconds; 60°C for 10 seconds; 72°C for 40 seconds) × 40 amplification cycles. Quantitative analysis of the resulting data was carried out using the $2^{-\Delta\Delta Ct}$ method.

Statistical analysis

Experimental data were analyzed using SPSS version 23.0 for further evaluation. Measurement data were assessed for normality. Data conforming to a normal distribution were presented as the mean ± standard deviation ($\bar{x} \pm s$). For comparisons among multiple groups, a one-way analysis of variance (ANOVA) was employed. In cases where the assumption of homogeneity of variances was satisfied, the least significant difference (LSD) test was used. Conversely, when variance heterogeneity was detected, Dunnett's T3 test was utilized as an alternative approach. Data that did not follow a normal distribution were represented using the median along with the interquartile range (median [P_{25}, P_{75}]). Comparisons between groups in such cases were performed using the nonparametric Kruskal–Wallis H test. All statistical evaluations were conducted as two-tailed tests, with a significance threshold set at $\alpha = 0.05$. Results yielding a P value less than 0.05 were interpreted as statistically significant.

Results

Effect of P2X7R KO on NF-κB p65 protein expression in UC mice

Observation of general conditions of mice in each group

In the WT-NC and P2X7R KO-NC groups, mice exhibited moderate body size, normal dietary and water consumption, moderately firm feces, and clean perianal regions. Conversely, in the WT-UC group, mice showed reduced body size, decreased food and water intake, loose and unformed stools with traces of blood, and perianal soiling from the third to fourth day of modeling. However, the P2X7R KO-UC group showed no abnormalities in body size, diet, water intake, or perianal cleanliness.

Histopathological observation of colon tissue of mice in each group

Histological examination using HE staining demonstrated marked variations in colon tissue pathology across the different experimental groups. In both the WT-NC and P2X7R KO-NC groups, the architecture of the colonic mucosa remained intact, characterized by preserved epithelial integrity, regularly aligned glands, and no signs of edema, congestion, or infiltration by inflammatory cells. In contrast, the WT-UC group showed significant epithelial defects, loss of some glandular structures, extensive ulcer formation, and substantial infiltration of inflammatory cells within both the mucosal and submucosal compartments. In the P2X7R KO-UC group, the mucosal epithelium appeared more intact, showing better-preserved mucosal structure and only slight inflammatory cell infiltration observed in both the mucosal and submucosal layers (Figure 1B). Compared to the WT-NC group, colon histopathology scores were significantly higher in the WT-UC group ($P < 0.05$). Meanwhile, the scores in the P2X7R KO-UC group were significantly lower than those in the WT-UC group ($P < 0.05$) (Figure 1C).

Observation of colonic goblet cells and intestinal mucus of mice in each group

In WT-NC and P2X7R KO-NC groups, crypts exhibited distinct structures with regular morphologies. Goblet cells are abundant within the crypts and actively secrete mucin, which forms a continuous and complete mucus layer covering the colonic epithelial surfaces. In contrast, almost all goblet cells disappeared from the crypts of the WT-UC group, leaving a severely damaged mucus layer. In the P2X7R KO-UC group, the crypt structures remained prominent and regular, with substantial goblet cell presence and active mucin secretion, contributing to improved mucus layer integrity (Figure 2).

NF-κB p65 protein expression in colon tissue of mice in each group

Compared to the WT-NC group, mice in the WT-UC group exhibited a notable elevation in NF-κB p65 expression level within colonic tissues ($P < 0.05$). In contrast, mice in the P2X7R KO-UC group showed a significant reduction in NF-κB p65 protein expression relative to those in the WT-UC group ($P < 0.05$) (Figure 3).

Study on the effect of moxibustion intervention on P2X7R/NF-κB pathway in UC rats

Observations on the general conditions of rats in each group

Throughout the modeling phase, animals in the normal group demonstrated normal dietary and water intake,

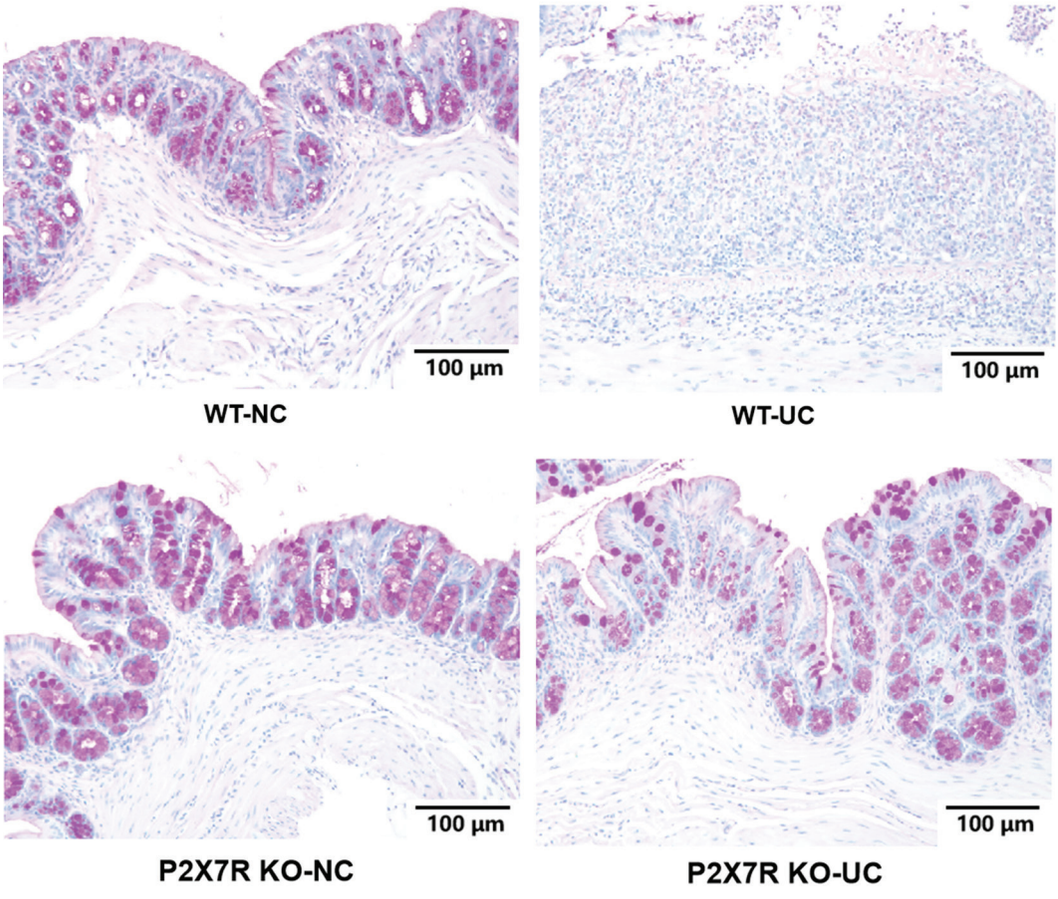


Figure 2. PAS staining of mice colon tissue in each group (scale bar = 100 μm). P2X7R: P2X7 receptor; P2X7R KO-NC: P2X7R gene knockout normal group; P2X7R KO-UC: P2X7R gene knockout model group; PAS: Periodic acid-Schiff; WT-NC: Wild-type normal group; WT-UC: Wild-type model group.

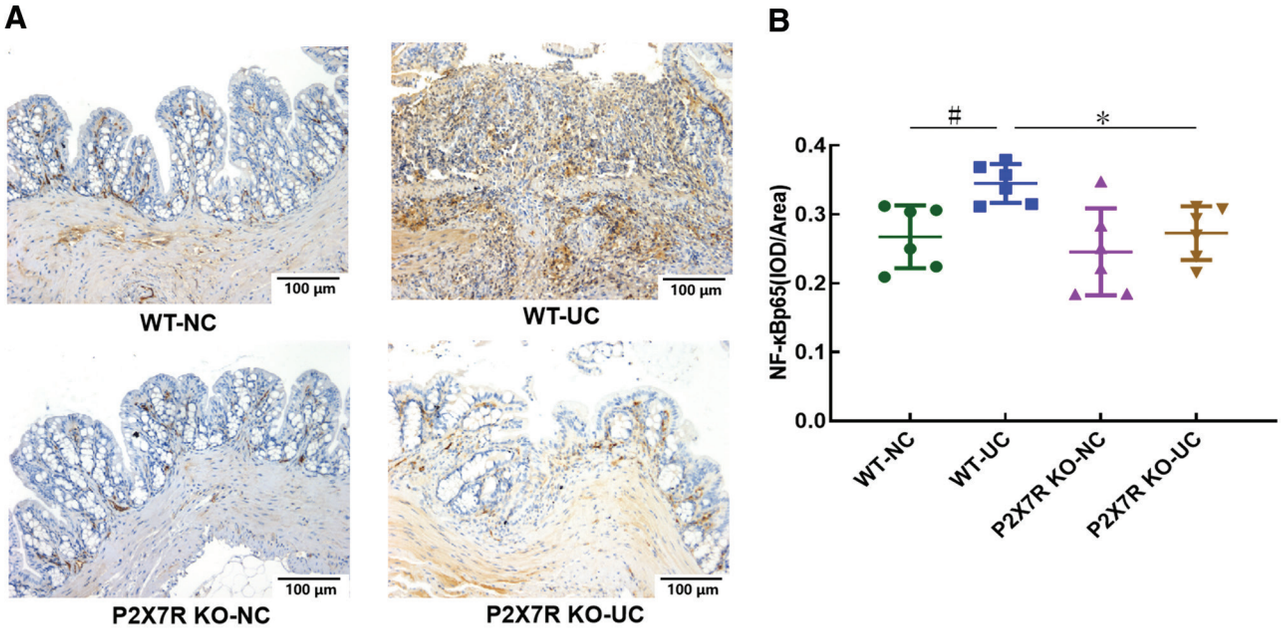


Figure 3. NF-κB p65 protein expression of mice colon tissue (scale bar = 100 μm). (A) NF-κB p65 protein expression of mice colon tissue in each group. (B) Quantitative analysis for NF-κB p65 protein ($\bar{x} \pm s$, $n = 6$). Compared with the WT-NC group, $^{\#}P < 0.05$; with the WT-UC group, $^{*}P < 0.05$. NF-κB: Nuclear factor-kappa B; P2X7R: P2X7 receptor; P2X7R KO-NC: P2X7R gene knockout normal group; P2X7R KO-UC: P2X7R gene knockout model group; WT-NC: Wild-type normal group; WT-UC: Wild-type model group.

soft-to-firm feces, and clean perianal regions. In contrast, the model group showed reduced physical activity, a thin body shape, decreased dietary and water intake, soiled perianal areas, unformed feces, and traces of blood in the stool.

During the intervention period, rats in both the normal and normal + herb-partitioned moxibustion groups showed no observable abnormalities. However, rats in the untreated model group remained thin, continued to produce loose stools, and had soiled perianal areas. The model + herb-partitioned moxibustion group displayed marked improvements in general conditions, including increased dietary intake, gradual normalization of stool formation, and cleaner perianal regions.

Effects of moxibustion on the histopathology of colon in UC rats

Under light microscopy, HE staining revealed clear differences in the mucosal integrity between the groups. Rats in the normal and normal + herb-partitioned moxibustion groups exhibited intact colonic epithelial tissue with well-arranged glands and defined mucosal structures. Capillaries and a few scattered lymphocytes were observed in the lamina propria without notable inflammatory cell infiltration, congestion, or edema. In contrast, colonic tissues from the model group displayed severe epithelial defects, poorly defined mucosal structures, extensive inflammatory cell infiltration within the mucosal and submucosal layers, glandular atrophy or disappearance, and ulcer formation. Meanwhile, rats in the model + herb-partitioned moxibustion group showed improved colonic mucosal structure with neoepithelial regeneration covering the defects. The glands were more regularly arranged than in the model group, and the ulcers had primarily healed, although inflammatory cell infiltration persisted within the mucosa and submucosa (Figure 4A). The colon histopathology scores of the rats in the model group were significantly higher than those in the normal group ($P < 0.05$). In contrast, the colon histopathology scores of rats in the model + herb-partitioned moxibustion group were significantly lower than those in the model group ($P < 0.05$). Additionally, no statistically significant difference was observed in the colon histopathology scores between the normal and normal + herb-partitioned moxibustion groups ($P > 0.05$) (Figure 4B).

Effects of moxibustion on goblet cells and intestinal mucus in colon tissue of UC rats

PAS staining highlighted distinct changes in goblet cell morphology and mucus secretion across the groups. The crypt morphology was well preserved in both the normal and normal + herb-partitioned moxibustion groups, with abundant goblet cells secreting large quantities of intestinal mucus. In contrast, crypts in the model group were distorted and atrophied with an irregular surface; goblet cells varied greatly in size, with a marked reduction in mucus secretion. In the model + herb-partitioned moxibustion group, the crypt structure was restored to a more regular shape, with increased goblet cell density and enhanced intestinal mucus secretion (Figure 5A).

Effect of moxibustion on IL-10 mRNA expression in colon tissue of UC rats

Compared to the normal group, IL-10 mRNA expression in colonic tissue was reduced in the model group rats; however, this reduction did not reach statistical significance ($P > 0.05$). In contrast, rats treated with herb-partitioned moxibustion showed an elevation in IL-10 mRNA expression compared to the model group, though the increase was not statistically meaningful ($P > 0.05$). Additionally, there was no notable statistical variation in IL-10 mRNA expression when comparing

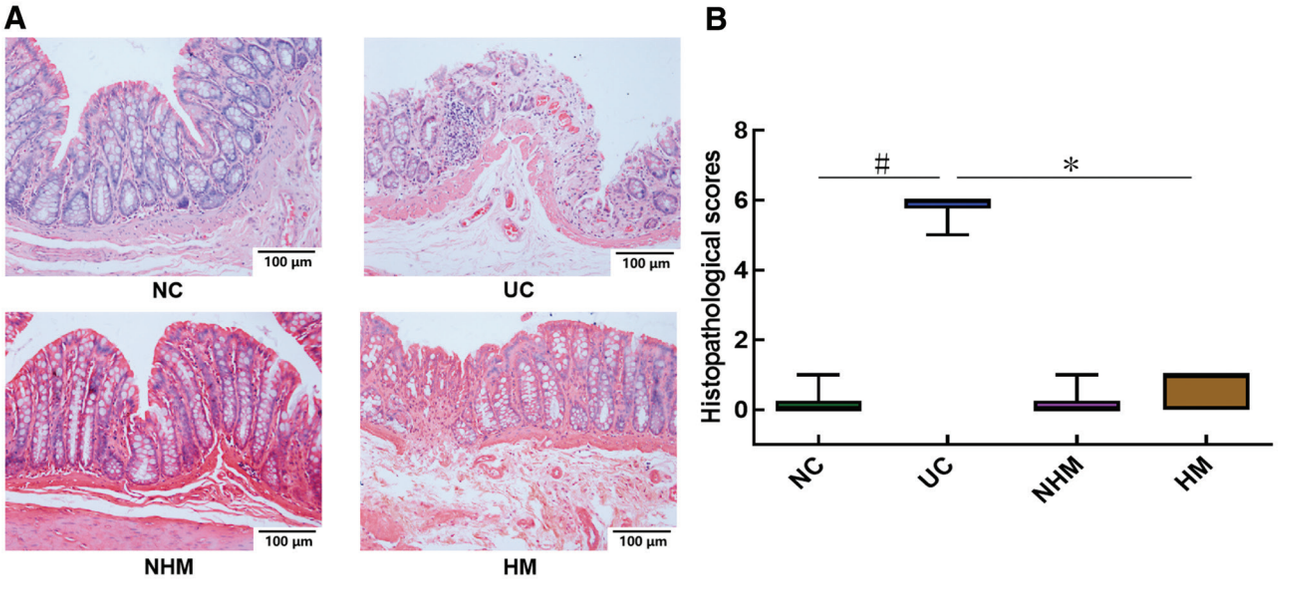


Figure 4. Histopathological observation of rats' colon tissue in each group (scale bar = 100 μm). (A) HE staining of rats' colon tissue in each group (scale bar = 100 μm); (B) Histopathologic scores of rats' colon tissue in each group (median [P_{25}, P_{75}], $n = 6$). Compared with the normal group, $^{\#}P < 0.05$; with the model group, $^{*}P < 0.05$. HE: Hematoxylin and eosin; HM: Model + herb-partitioned moxibustion group; NC: Normal group; NHM: Normal + herb-partitioned moxibustion group; UC: Ulcerative colitis (model group).

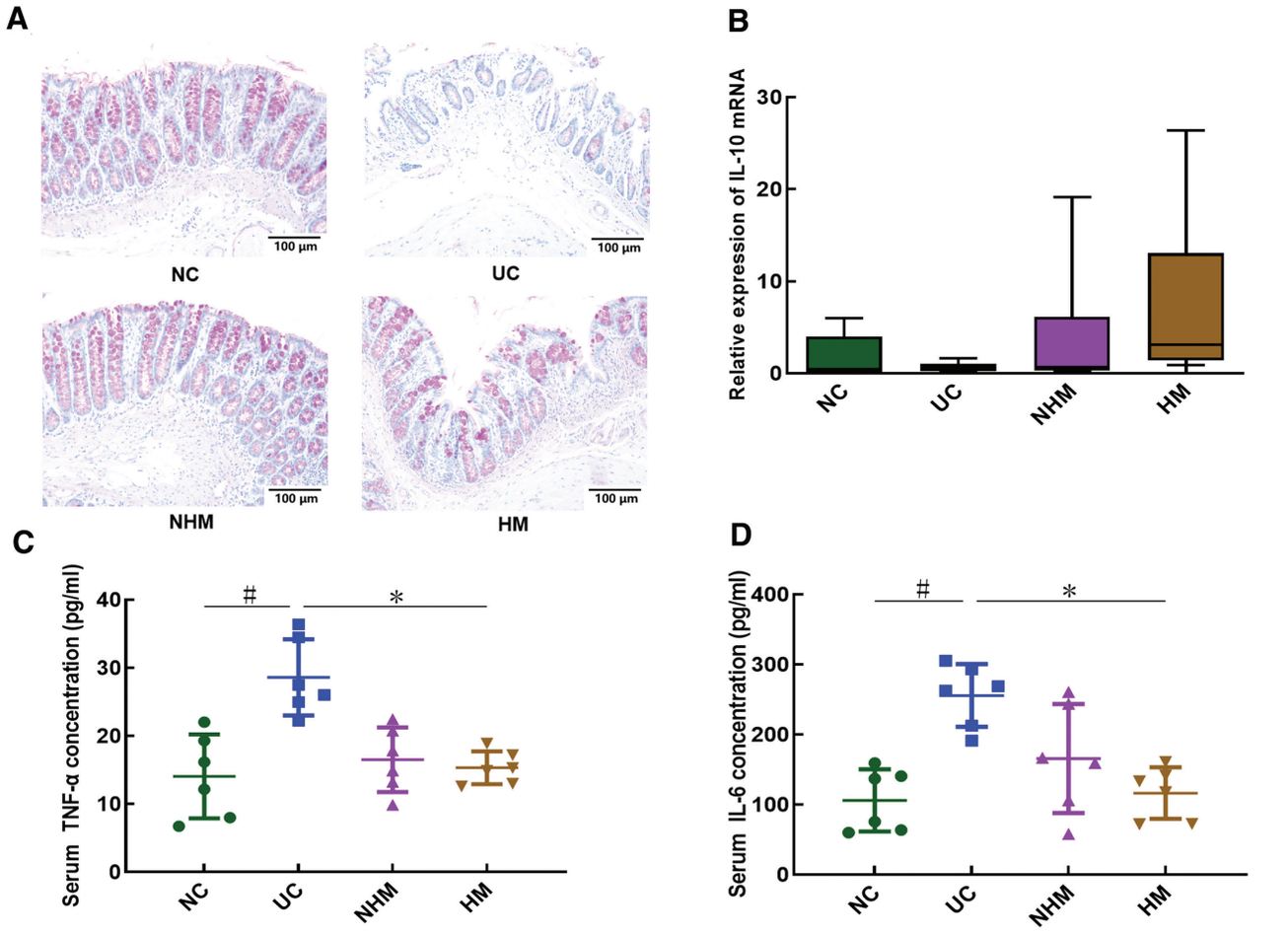


Figure 5. PAS staining of rats colon tissue, expression of IL-10 mRNA in colon tissue and serum TNF-α and IL-6 concentrations of rats. (A) PAS staining of rats colon tissue in each group (scale bar = 100 μm). (B) Expression of IL-10 mRNA in colon tissue of rats in various groups ($\bar{x} \pm s$, $n = 6$). (C– D) Serum TNF-α and IL-6 concentrations of rats in each group ($\bar{x} \pm s$, $n = 6$). Compared with the normal group, $^{\#}P < 0.05$; with the model group, $^{*}P < 0.05$. HM: Model + herb-partitioned moxibustion group; IL: Interleukin; NC: Normal group; NHM: Normal + herb-partitioned moxibustion group; PAS: Periodic acid-Schiff; TNF: Tumor necrosis factor; UC: Ulcerative colitis (model group).

the normal group with the normal + herb-partitioned moxibustion group ($P > 0.05$) (Figure 5B).

Effects of moxibustion on serum TNF-α and IL-6 concentrations in UC rats

Compared to the normal group, the serum concentrations of TNF-α and IL-6 in the rat model group were significantly increased ($P < 0.05$). In contrast, the serum TNF-α and IL-6 concentrations of rats in the model + herb-partitioned moxibustion group were significantly reduced compared to the model group ($P < 0.05$). Additionally, there was no notable statistical variation in serum TNF-α and IL-6 concentrations when comparing the normal group with the normal + herb-partitioned moxibustion group ($P > 0.05$) (Figure 5C and D).

Effect of moxibustion on P2X7R protein expression in colon tissue of UC rats

IHC detection showed positive expression of the P2X7R protein as brown-colored staining in colonic tissues. Only low levels of P2X7R expression were detected within the cytoplasm of glandular epithelial cells in both the normal and normal + herb-partitioned moxibustion groups. However, strong P2X7R expression was evident in the model group, with a deep staining intensity and dense distribution throughout the glandular epithelial cells. In comparison, although positive, P2X7R expression levels were reduced in the colonic tissues of the model + herb-partitioned moxibustion group (Figure 6A). The model group exhibited a marked elevation in P2X7R expression within colonic tissue relative to the normal group ($P < 0.05$). In contrast, rats receiving herb-partitioned moxibustion showed a notable decline in P2X7R levels in the colon when compared with the model group ($P < 0.05$). Additionally, there was no notable statistical variation in P2X7R expression when comparing the normal group with the normal + herb-partitioned moxibustion group ($P > 0.05$) (Figure 6C).

Effects of moxibustion on NF-κB p65 protein expression in rat colon tissues of each group

Positive expression of NF-κB p65 protein was similarly detected in brown-stained areas under light microscopy. NF-κB p65 protein expression was minimal in the glandular epithelial cells of rats from the normal and normal + herb-partitioned moxibustion groups. In contrast,

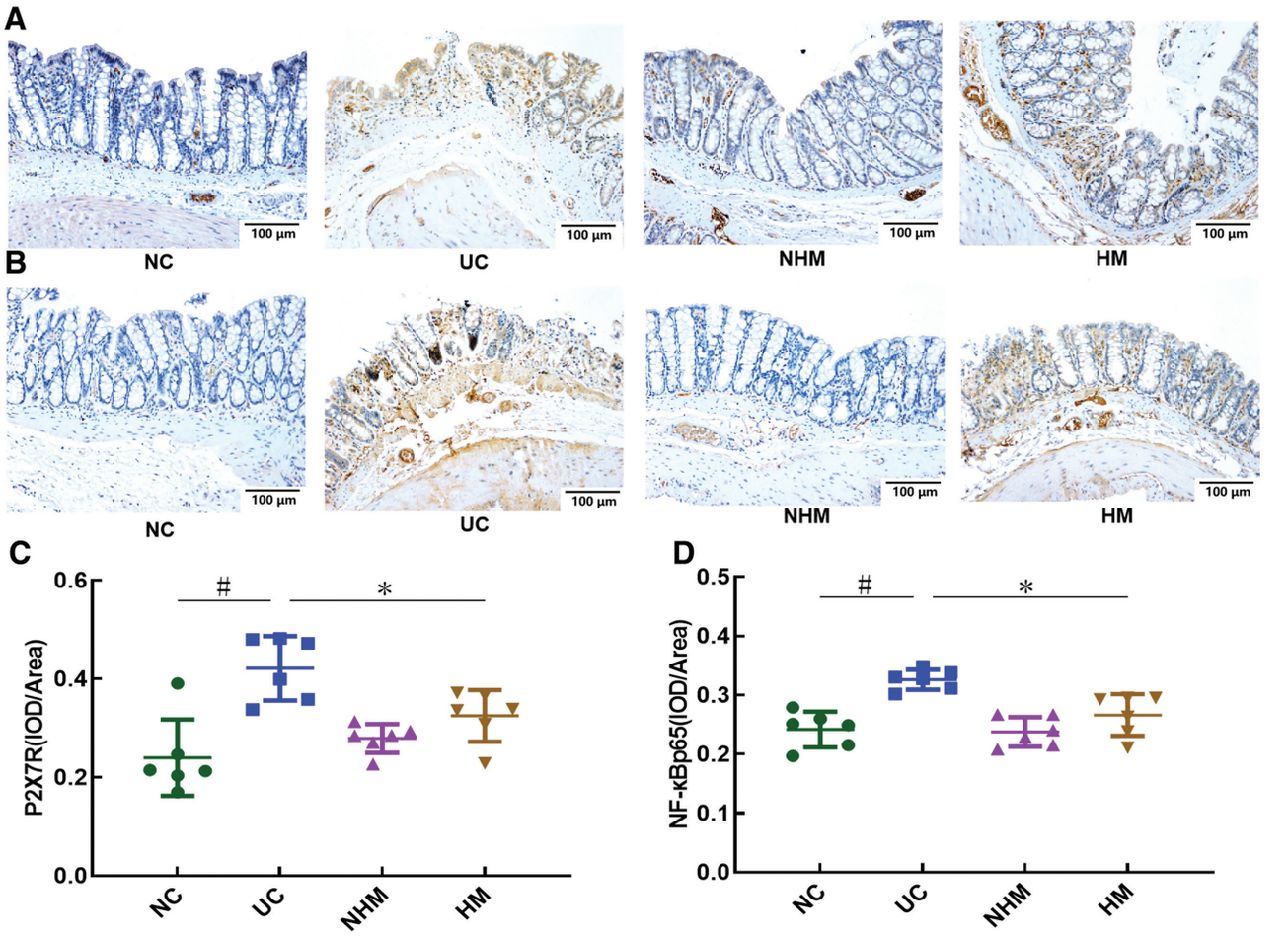


Figure 6. P2X7R and NF-κB p65 protein expressions of rats' colon tissue (scale bar = 100 μm). (A) P2X7R protein expression of rats' colon tissue in each group ($\bar{x} \pm s$, $n = 6$); (B) NF-κB p65 protein expression of rats' colon tissue in each group ($\bar{x} \pm s$, $n = 6$); (C) Quantitative analysis for P2X7R protein; (D) Quantitative analysis for NF-κB p65 protein. Compared with the normal group, $^{\#}P < 0.05$; with the model group, $^{*}P < 0.05$. HM: Model + herb-partitioned moxibustion group; NC: Normal group; NF-κB: Nuclear factor-kappa B; NHM: Normal + herb-partitioned moxibustion group; P2X7R: P2X7 receptor; UC: Ulcerative colitis (model group).

NF-κB p65 protein levels were significantly elevated in rats from the model group with strongly positive staining concentrated within both cytoplasm and nuclei of glandular epithelial cells. Notably, NF-κB p65 protein expression levels were reduced but remained variably positive within the colonic nuclei of rats in the model + herb-partitioned moxibustion group (Figure 6B).

The model group exhibited a marked elevation in NF-κB p65 expression within colonic tissue relative to the normal group ($P < 0.05$). In contrast, rats receiving herb-partitioned moxibustion showed a notable decline in NF-κB p65 levels in the colon when compared with the model group ($P < 0.05$). Additionally, there was no notable statistical variation in NF-κB p65 expression when comparing the normal group with the normal + herb-partitioned moxibustion group ($P > 0.05$) (Figure 6D).

Discussion

The DSS-induced colitis model is widely recognized for its simplicity, reproducibility, and ability to replicate epithelial damage observed in human UC[23]. The success of this model depends on factors such as DSS concentration and molecular weight. Depending on administration frequency and duration, animals can develop acute or chronic colitis[24]. Chronic DSS-induced UC models have pathology comparable to the relapsing nature of human UC[25]. In the present study, we successfully established a rat model of chronic UC using repeated DSS induction cycles. Rats in the model group exhibited the typical histopathological features of colonic damage, including epithelial defects, loss of glandular integrity, ulcer formation, and mucosal/submucosal inflammatory infiltration. PAS staining revealed crypt atrophy, distortion, goblet cell depletion, and reduced mucus secretion. Interestingly, the histopathological findings in the acute DSS-induced mouse model were similar to those observed in the chronic rat model.

P2X7R is closely associated with the regulation of inflammation[15]. When activated by inflammatory stimuli, P2X7R triggers NF-κB activation through the MAPK pathway by inducing IκB phosphorylation and ubiquitination. This process leads to proteasomal degradation of IκB inhibitors and nuclear translocation of NF-κB[26], binding specific DNA sites to induce pro-inflammatory gene transcription. Key cytokines (eg, TNF-α and IL-6) subsequently activate NF-κB in a positive feedback loop that amplifies inflammation. NF-κB also orchestrates pro-survival functions in intestinal epithelial cells while

inducing pro-inflammatory cascades in innate and adaptive immune responses. Emerging evidence highlights the contribution of both P2X7R and NF-κB to regulating inflammatory pathways. In IBD animal models, their expression levels are upregulated, and their interplay through the P2X7R/NF-κB axis has been recognized as a key driver of IBD pathogenesis[27–28]. The roles of P2X7R and NF-κB in UC involve the intricate regulation of cellular signaling pathways, where both molecules play pivotal roles in modulating immune responses, inflammatory cascades, and epithelial barrier function. Activation of P2X7R frequently coincides with NF-κB pathway activation. For instance, the activation of P2X7R promotes the formation of the NLRP3 inflammasome, leading to the release of IL-1β, which further amplifies NF-κB activity *via* autocrine and paracrine mechanisms, thereby intensifying the pro-inflammatory response. NF-κB is recognized as a key regulatory factor involved in the development and progression of UC[29]. Importantly, the inhibition of P2X7R has been shown to disrupt NF-κB nuclear translocation, underscoring their functional association[30]. Moreover, studies have suggested that P2X7R promotes the production of inflammatory cytokines by activating, rather than inactivating, the NF-κB pathway. This dysregulation exacerbates DSS-induced colitis by increasing the intestinal mucosal barrier[27]. The combined actions of P2X7R and NF-κB contribute to a progressive deterioration of the intestinal microenvironment by weakening epithelial barrier function, inducing immune imbalances, and perpetuating chronic tissue damage. This, in turn, facilitates the progression of IBD from the acute to chronic relapsing phases.

KO models have been widely used in biological and medical research to study disease mechanisms. Research has demonstrated that P2X7R KO mice exhibited protective effects against intestinal inflammation induced by TNBS or oxazolone[31]. This study investigated the colonic histopathological changes, goblet cell counts, and intestinal mucus secretion in DSS-induced acute colitis in P2X7R KO mice. The findings revealed that P2X7R KO mice displayed a significantly attenuated inflammatory response compared to their WT counterparts. Structural preservation of crypts with regular morphology, a higher count of goblet cells, and enhanced mucin secretion were observed in KO mice. These features suggest a mild degree of intestinal injury. Further analysis revealed that DSS-induced expression of NF-κB p65 protein in the colonic tissues of KO mice was significantly reduced compared to that in WT mice. This confirms the regulatory effect of P2X7R on NF-κB p65 expression. Consistent with these observations, in UC rats subjected to repeated DSS induction, the expression levels of P2X7R and the NF-κB p65 were significantly increased relative to those observed in the NC group. These findings indicate that the P2X7R/NF-κB signaling pathway is critically involved in the molecular mechanisms underlying the development of UC.

Acupuncture and moxibustion have shown therapeutic benefits in treating IBD as they regulate immune homeostasis through multi-target and multi-layered mechanisms[10,32–33]. Moxibustion intervention significantly reduced the abnormally high protein expression of P2X7R and NF-κB p65 observed in the colonic tissues of rats with UC. These findings indicate that the P2X7R/NF-κB pathway represents a critical signaling axis modulated by moxibustion during UC treatment. P2X7R is well-recognized as a crucial cell surface receptor involved in modulating the release of pro-inflammatory cytokines, such as TNF-α, IL-6, and IL-1β[34]. Cytokine homeostasis is essential for maintaining intestinal equilibrium; however, stimulation of the colonic mucosa disrupts cytokine balance, leading to immune dysregulation and exacerbation of intestinal injury[35]. Anti-inflammatory cytokines mitigate inflammation through immune-specific and non-immune mechanisms to stabilize the intestinal microenvironment. IL-10 plays a powerful immunoregulatory role by suppressing the synthesis of pro-inflammatory cytokines such as TNF-α, IL-6, and IL-1β, ultimately restoring cytokine balance[36]. Serum concentrations of TNF-α and IL-6 were significantly elevated in UC model rats compared to NCs in our study. Moxibustion treatment effectively reduced these cytokine levels, suggesting its potential to modulate inflammatory responses. However, the expression levels of IL-10 mRNA did not exhibit any statistically meaningful variation among the different experimental groups; this finding warrants further investigation at the protein level.

To evaluate the broader effects of moxibustion, we included a normal + herb-partitioned moxibustion group in our experimental design. The primary objective of this study was to assess whether moxibustion exerts any influence on the general physiological conditions or laboratory indices of healthy animals. The results showed no statistically significant differences between this group and the untreated NCs in terms of general conditions or laboratory parameters. These findings suggest that moxibustion does not cause toxic side effects in healthy individuals. This highlights the potential of moxibustion as a preventive healthcare measure for disease management and health preservation.

This study has several inherent limitations. First, although mouse and rat models are valuable experimental tools for understanding UC pathogenesis, they may not fully replicate human disease dynamics, particularly immune responses. Future studies should prioritize human-derived models (eg, organoids or primary biopsies) to increase the translational relevance. In this study, we used different rodent species because gene KO mouse models are more mature, and rat acupuncture points are relatively easy to locate, making it easier to perform medicinal moxibustion. Future research should integrate rat gene-editing technology to improve model consistency. Second, although our findings highlight the regulatory effects of moxibustion on the P2X7R/NF-κB axis in animal models, clinical studies are required to validate these observations in humans. Furthermore, inter-individual variability across patients necessitates caution when extrapolating the experimental findings directly to clinical practice.

Conclusion

In conclusion, this study demonstrates that P2X7R gene KO alleviates epithelial damage and inflammation in UC

by suppressing NF-κB signaling. Additionally, moxibustion treatment significantly reduces serum TNF-α and IL-6 levels while down-regulating P2X7R and NF-κB p65 expression in colon tissues from DSS-induced UC rats. These findings suggest that moxibustion inhibits intestinal inflammation by modulating the P2X7R/NF-κB pathway and influencing cytokine levels. Future studies should explore the therapeutic mechanisms of moxibustion using clinical trials or more advanced *ex vivo* models.

Conflict of interest statement

The authors declare no conflict of interest.

Funding

This research was funded by the National Natural Science Foundation of China (82174501, 82105012, 82205293, 82205262), Shanghai Municipal Natural Science Foundation (22ZR1458400), Shanghai Talent Development Fund Project (2021058), Shanghai University of Traditional Chinese Medicine Science and Technology Development Project (23KFL111), State Administration of Traditional Chinese Medicine high-level key discipline construction project (zyyzdxk-2023068).

Author contributions

Yanan Liu and Yu Qiao contributed to data curation; Huangan Wu and Luyi Wu contributed to funding acquisition; Yaying Lin, Shiyu Zheng, and Ling Yang contributed to investigation; Yan Huang contributed to resources; Fang Zhang contributed to software; Qin Qi and Jianhua Zhou contributed to supervision; Zhe Ma and Lingjie Li contributed to writing–original draft; Lu Zhu contributed to writing–review & editing. All authors have read and agreed to the published version of the manuscript.

Ethical approval of studies and informed consent

All animal procedures performed in this study were reviewed, approved, and supervised by the Animal Ethics Committee of Shanghai University of Traditional Chinese Medicine, ensuring strict adherence to ethical standards and animal welfare guidelines (Approval number: PZSHUTCM211227012).

Acknowledgments

None.

Data availability

All data generated or analyzed during this study are included in this published article.

References

[1] Rubin DT, Ananthakrishnan AN, Siegel CA, et al. ACG clinical guideline: ulcerative colitis in adults. *Am J Gastroenterol* 2019;114(3):384–413.
[2] Shi R, Li JX, Shen H, et al. Experts consensus on traditional Chinese medicine diagnosis and treatment of ulcerative colitis (2023). *CJTCMP* 2024;39(1):288–296.
[3] Wei SC, Sollano J, Hui YT, et al. Epidemiology, burden of disease, and unmet needs in the treatment of ulcerative colitis in Asia. *Expert Rev Gastroenterol Hepatol* 2021;15(3):275–289.
[4] Le Berre C, Honap S, Peyrin-Biroulet L. Ulcerative colitis. *Lancet* 2023;402(10401):571–584.
[5] Du L, Ha C. Epidemiology and pathogenesis of ulcerative colitis. *Gastroenterol Clin North Am* 2020;49(4):643–654.
[6] Le Berre C, Ananthakrishnan AN, Danese S, et al. Ulcerative colitis and Crohn's disease have similar burden and goals for treatment. *Clin Gastroenterol Hepatol* 2020;18(1):14–23.
[7] Allen PB, Bonovas S, Danese S, et al. Evolving primary and secondary endpoints in randomized controlled trials leading to approval of biologics and small molecules in IBD: an historical perspective. *Expert Opin Biol Ther* 2020;20(2):151–161.
[8] Zhou EH, Liu HR, Wu HG, et al. Down-regulation of protein and mRNA expression of IL-8 and ICAM-1 in colon tissue of ulcerative colitis patients by partition-herb moxibustion. *Dig Dis Sci* 2009;54(10):2198–2206.
[9] Wu HG, Shi Z, Zhu Y, et al. Clinical study on the treatment of ulcerative colitis by spacer moxibustion. *Shanghai Acupunct Moxibustion J* 2007;26(4):3–4.
[10] Qi Q, Im H, Li KS, et al. Influence of herb-partitioned moxibustion at Qihai (CV6) and bilateral Tianshu (ST25) and Shangjuxu (ST37) acupoints on toll-like receptors 4 signaling pathways in patients with ulcerative coliti. *J Tradit Chin Med* 2021;41(3):479–485.
[11] Zhao JM, Wu HG, Lu Y, et al. Herb-partition moxibustion relieve colonic inflammation in ulcerative colitis of DDS-induced rats *via* dual inhibition of NF-κB and STAT3 activation. *World Sci Technol Modern Tradit Chin Med Mater Med* 2018;20(9):1579–1584.
[12] Ma Z, Fang ZZ, Wu HG, et al. Protective mechanism of preventative moxibustion at tianshu acupoint (ST25) on intestinal barrier in UC rats. *World Sci Technol Modern Tradit Chin Med Mater Med* 2018;20(9):1555–1563.
[13] Di Virgilio F. P2X receptors and inflammation. *Curr Med Chem* 2015;22(7):866–877.
[14] Surprenant A, North RA. Signaling at purinergic P2X receptors. *Annu Rev Physiol* 2009;71:333–359.
[15] Neves AR, Castelo-Branco MT, Figliuolo VR, et al. Overexpression of ATP-activated P2X7 receptors in the intestinal mucosa is implicated in the pathogenesis of Crohn's disease. *Inflamm Bowel Dis* 2014;20(3):444–457.
[16] Marques CC, Castelo-Branco MT, Pacheco RG, et al. Prophylactic systemic P2X7 receptor blockade prevents experimental colitis. *Biochim Biophys Acta* 2014;1842(1):65–78.
[17] Huang C, Chi XS, Li R, et al. Inhibition of P2X7 receptor ameliorates nuclear Factor-Kappa B mediated neuroinflammation induced by status epilepticus in rat hippocampus. *J Mol Neurosci* 2017;63(2):173–184.
[18] Chen L, Wang H, Xing J, et al. Silencing P2X7R alleviates diabetic neuropathic pain involving TRPV1 *via* PKCε/P38MAPK/NF-κB signaling pathway in rats. *Int J Mol Sci* 2022;23(22):14141.
[19] Fang ZZ, Wu HG, Wu LY, et al. Exploring the mechanism by which acupuncture and moxibustion reduce colonic mucosal inflammation in rats with ulcerative colitis (UC) based on the P2X7R-NLRP3 inflammasome pathway. *J Acupunct Tuina Sci* 2023;21(5):356–367.
[20] Huang Y, Ma Z, Cui YH, et al. Effects of herb-partitioned moxibustion on the miRNA expression profiles in colon from rats with DSS-Induced ulcerative colitis. *Evid Based Complement Alternat Med* 2017;2017:1767301.
[21] Greten FR, Eckmann L, Greten TF, et al. IKKbeta links inflammation and tumorigenesis in a mouse model of colitis-associated cancer. *Cell* 2004;118(3):285–296.
[22] Li G, Zhao C, Xu J, et al. Moxibustion alleviates intestinal inflammation in ulcerative colitis rats by modulating long non-coding RNA LOC108352929 and inhibiting Phf11 expression. *Heliyon* 2024;10(5):e26898.
[23] Chassaing B, Aitken JD, Malleshappa M, et al. Dextran sulfate sodium (DSS)-induced colitis in mice. *Curr Protoc Immunol* 2014;104:15.25.1–15.25.14.
[24] Eichele DD, Kharbanda KK. Dextran sodium sulfate colitis murine model: an indispensable tool for advancing our understanding of inflammatory bowel diseases pathogenesis. *World J Gastroenterol* 2017;23(33):6016–6029.
[25] Zhao SS, Huang X, Qin MB, et al. Establishment and evaluation of chronic ulcerative colitis mice model induced by dextran sodium sulfate. *J GuangXi Med Univ* 2019;36(4):559–562.

[26] Gavala ML, Pfeiffer ZA, Bertics PJ. The nucleotide receptor P2RX7 mediates ATP-induced CREB activation in human and murine monocytic cells. *J Leukoc Biol* 2008;84(4):1159–1171.
[27] Wan P, Liu X, Xiong Y, et al. Extracellular ATP mediates inflammatory responses in colitis *via* P2 × 7 receptor signaling. *Sci Rep* 2016;6:19108.
[28] Liu Y, Xiao J, Zhao X, et al. Inhibiting ATP/P2X7R signaling protects intestinal barrier in dextran sulfate sodium-induced colitis and Crohn's disease through inactivating NF-κB pathway in macrophages. *Chin Med J (Engl)* 2023;136(12):1506–1508.
[29] Zhang Y, Tao M, Chen C, et al. BAFF blockade attenuates DSS-induced chronic colitis *via* inhibiting NLRP3 inflammasome and NF-κB activation. *Front Immunol* 2022;13:783254.
[30] Tafani M, Schito L, Pellegrini L, et al. Hypoxia-increased RAGE and P2X7R expression regulates tumor cell invasion through phosphorylation of Erk1/2 and Akt and nuclear translocation of NF-κB. *Carcinogenesis* 2011;32(8):1167–1175.
[31] Figliuolo VR, Savio LEB, Safya H, et al. P2X7 receptor promotes intestinal inflammation in chemically induced colitis and triggers death of mucosal regulatory T cells. *Biochim Biophys Acta Mol Basis Dis* 2017;1863(6):1183–1194.
[32] Bao CH, Zhang JR, Wu HG. Acupuncture for Crohn's disease: current status and future perspectives. *Acupunct Herb Med* 2023;3(4):229–231.
[33] Wu HG, Wu LY. Research progress and key scientific problems of traditional Chinese moxibustion. *Acupunct Herb Med* 2024;4(1):16–18.
[34] Lister MF, Sharkey J, Sawatzky DA, et al. The role of the purinergic P2X7 receptor in inflammation. *J Inflamm (London, England)* 2007;4:5.
[35] Strober W, Fuss IJ. Proinflammatory cytokines in the pathogenesis of inflammatory bowel diseases. *Gastroenterology* 2011;140(6):1756–1767.
[36] Kole A, Maloy KJ. Control of intestinal inflammation by interleukin-10. *Curr Top Microbiol Immunol* 2014;380:19–38.